

Identifications and in silico analysis of a spectrum of SLC4A11 mutations in Indian familial and non-familial cases of congenital hereditary endothelial dystrophy

Mohd Salman

LV Prasad Eye Institute

Anshuman Verma (✉ vermaamrf@gmail.com)

MNR Medical College and Hospital <https://orcid.org/0000-0003-0948-0154>

Sunita Chaurasia

LV Prasad Eye Institute

Deeksha Prasad

LV Prasad Eye Institute

Chitra Kannabiran

LV Prasad Eye Institute

Vivek Singh

LV Prasad Eye Institute

MURALIDHAR RAMAPPA

LV Prasad Eye Institute <https://orcid.org/0000-0003-3667-5483>

Research Article

Keywords: CHED, SLC4A11, Corneal dystrophy, Mutations

Posted Date: May 13th, 2022

DOI: <https://doi.org/10.21203/rs.3.rs-1623088/v1>

License:  This work is licensed under a Creative Commons Attribution 4.0 International License.

[Read Full License](#)

Title – Identifications and in silico analysis of a spectrum of *SLC4A11* mutations in Indian familial and non-familial cases of congenital hereditary endothelial dystrophy

Authors: Mohd Salman^{¶1,2}, Anshuman Verma^{¶1,3}, Sunita Chaurasia³, Deeksha Prasad^{1,2}, Chitra Kannabiran³, Vivek Singh^{*1}, Muralidhar Ramappa^{*4,5,6}

Affiliations: ¹Prof. Brien Holden Eye Research Center, Champalimaud Translational Centre for Eye Research, L V Prasad Eye Institute, Hyderabad, India. ²Manipal Academy of Higher Education, Manipal, Karnataka, India. ³MNR Foundation for Research and Innovations, MNR Medical College, MNR Nagar, Sangareddy, Telangana, India. ⁴Centre for Rare Eye Diseases and Ocular Genetics, L V Prasad Eye Institute, Hyderabad, India. ⁵Jasti V Ramanamma Children's Eye Care Center, L V Prasad Eye Institute, Hyderabad, India. ⁶The Cornea Institute, L V Prasad Eye Institute, Hyderabad, India.

¶ These authors contributed equally to this work

***Correspondence to:**

Muralidhar Ramappa

Clinician Scientist & Senior Ophthalmologist,

Cornea and Anterior Segment, L V Prasad Eye Institute,

KAR Campus, Banjara Hills, Hyderabad, India

E-mail: muralidhar@lvpei.org

Vivek Singh

Senior scientist, Prof. Brien Holden Eye Research Center,

Champalimaud Translational Centre for Eye Research,

L V Prasad Eye Institute, Hyderabad, India E-mail: viveksingh@lvpei.org

Abstract

Background: Congenital hereditary endothelial dystrophy (CHED) is a rare form of corneal dystrophy and is known to be caused by *SLC4A11* gene mutation. The purpose of this study is to find genetic alterations in *SLC4A11* using direct sequencing in two Indian familial CHED cases with affected members n=3 and n=2 respectively and five non-familial cases with a single affected member, followed by in silico characterization of identified mutations.

Results: All three affected members of the first CHED family were identified with novel hom. c.1514C>G (p.Ser489Trp) mutation while second family showed presence of novel compound heterozygous mutation- het c.529A>C (p.Arg161Arg) + het c.2461insT (p.Val805fs). Among five non-familial cases, two showed novel changes hom. c.1487G>T (p.Ser480Ile) and hom. c.620-2A>G respectively, while the other one had previously reported hom. c.2653C>T (p.Arg869Cys) mutation. The remaining two cases did not reveal the presence of *SLC4A11* related pathogenic mutations. Identified mutations were excluded from a large number of controls (n=80) and analyzed in silico using homology-based protein modeling and pathogenicity prediction tools, which predicted these alterations to be pathogenic causing change in protein stability, protein local flexibility and decrease in hydrogen bond interactions.

Conclusions: Our study contributed to CHED mutational spectrum adding four novel mutations and confirming a previously reported mutation. Our study demonstrated a spectrum of mutations ranging from coding, non-coding, homozygous, and synonymous compound heterozygous in CHED cases. The identified mutations demonstrated different degrees of pathogenic effects based on in silico analysis. In addition, two non-familial cases could not be identified with pathogenic mutation emphasizing the involvement of other genes or genetic mechanisms for such cases.

Key words: CHED, SLC4A11, Corneal dystrophy, Mutations

Background

Congenital hereditary endothelial dystrophy (CHED) [MIM: 217700] is rare corneal dystrophy and holds a significant indication of corneal transplantation in India and middle east countries[1]. The disease involves dysfunction of corneal endothelium that leads to presenile senescence of corneal endothelial cells with thickened Descemet membrane and progressive corneal clouding in the early stages of life. Varying degrees of amblyopia, nystagmus, and glaucomatous features may appear in patients in advanced stages of the disease [2]. The identification of the genetic cause of CHED historically started using linkage analysis in British familial cases describing its two forms, CHED-1 (autosomal dominant) and CHED-2 (autosomal recessive), with a common genetic locus, which in later studies got distinguished as two separate loci. Eventually, a study by Vithana et al. in a consanguineous family from Myanmar refined CHED2 locus and confirmed the underlying genetic factor '*SLC4A11*' as a prime candidate gene [3]. Subsequent studies further recapitulated these findings, and many *SLC4A11* mutations were reported (**Supplementary Table 1**), enabling *SLC4A11* as an established causative gene for CHED2. In addition, the *SLC4A11* K/O mice also corroborate with the CHED phenotype confirming the role of *SLC4A11* in disease pathogenesis [4]. In the current international classification of corneal dystrophy (IC3D), CHED 2 is identified as an autosomal recessive form of corneal endothelial dystrophies or simply CHED, while CHED1 is now recognized as a posterior polymorphous corneal dystrophy (PPCD) or posterior polymorphous dystrophy (PPMD), part of an autosomal dominant form of corneal endothelial dystrophies [5]. *SLC4A11* gene, located on chromosome 20p13, encodes for a transmembrane sodium bicarbonate transporter-like protein-11. On the corneal endothelial surface, it acts as a “pump” to transport of ions across endothelium to corneal stroma. It facilitates the propelling of

water from stroma to aqueous humor, maintaining a dehydrated state of the corneal stroma [6]. Apart from CHED, a mutation in *SLC4A11* is also known to cause some form of autosomal dominant Fuch corneal endothelial dystrophy (FECD) and Harboyan syndrome (HS) or corneal dystrophy-perceptive deafness (CDPD) [7]. There is an overlap of the clinical CHED phenotype with primary congenital glaucoma, and PPCD, whose genetic origins are different. The *SLC4A11* mutational screening can be helpful in differential diagnosis and currently available corneal transplant management in the form of DSEK/DMEK [8]. Certain *SLC4A11* SNPs have been reported to be linked with Bisphenol-A (BPA) induced ovarian carcinoma [9]. Specific non-steroidal anti-inflammatory drugs (NSAIDs) are being tested for their potential in correcting *SLC4A11* specific mutant effects [10]. *SLC4A11* mutational spectrum will be required for developing such medicinal approaches and emerging regenerative medicine such as gene therapy or CRISPR-based gene editing therapy [11-13]. Screening of familial CHED cases can also help to measure the risk and management of the disease. In this study, we have analysed two familial cases of CHED having multiple affected members and five non-familial cases with a single proband, screening all coding exons with flanking intronic region of *SLC4A11* gene using the direct sequencing method. We also characterized the identified mutations in silico using homology modeling and pathogenicity prediction tools and looked at the disease phenotype.

Methods

Ethics statement: The study was approved by the institutional review board of the L V Prasad Eye Institute (Ethics Ref. No. LEC-BHR-01-20-381) and followed the tenets of the declaration of Helsinki.

Subjects and clinical examination: Patients were recruited in L V Prasad Eye hospital, India, between 2007-2021. The informed consent for the study was approved by each participant or their

guardian in case of a minor. The demographic and clinical details of subjects are given in **Table1**. The diagnosis of the diseases was based on the ground glass corneal clouding in the presence of normal anterior segment architecture. All the patients had a detailed ophthalmic examination. An increase in corneal thickness due to edema was measured using OCT (RTVue-100 FD-OCT (Optovue, Fremont, California, USA) (**Fig.1**). The pedigrees were constructed for each proband based on the information provided by guardians (**Fig.2**). Eighty healthy controls were also recruited.

Genetic analysis: From each participant, 2-3mL of blood was drawn from a radial vein. The genomic DNA was extracted from blood samples using a DNA extraction kit (JetFlex™ Genomic DNA Purification Kit, A30700, Invitrogen). The 19 coding exons and flanking intronic regions of the corneal gene transcript *SLC4A11*-201 (NCBI reference sequence NM_032034.3) (Transcript ID ENST00000380056.7) were targeted using 13 sets of published and newly designed primers. PCR amplification of each amplicon was performed using EmeraldAmp MAX HS PCR Master Mix RR330, Takara, as per conditions described in **Supplementary Table.2**. The diluted (1/10th to 1/15th) amplified PCR product was subjected for Sanger sequencing using Big Dye Terminator ready reaction mix on an ABI-3130 XL sequence analyzer (Applied Biosystems). The sequence data analysis was done using tools such as CHROMAS, FINCH TV, APE, and location and position of identified variations was mapped against ENSEMBL genome browser <https://www.ensembl.org/>

In silico analysis: The identified variations were analyzed for their pathogenicity score using Predict SNP server <https://loschmidt.chemi.muni.cz/predictsnp> with a number of tools, including SIFT and PolyPhen. The provean (<http://provean.jcvi.org/>) server provided the similar deleterious score. The mutated residue conservation was analyzed with the ConSurf server

<https://consurf.tau.ac.il> (Table 4). As the crystal protein structure of *SLC4A11* is not yet solved, a homology-based modeling approach was executed for structural analysis. Using Modeller-10.1, a basic wild type (WD) three-dimensional homology model of the human *SLC4A11* trans-membrane domain was created, taking the crystal structure template of the anion exchanger domain of human erythrocyte band-3 domain at 3.5Å resolution (PDB 4YZF) having a percentage of sequence identity ~30% (Fig.3A). The structure validation was done using SAVES-v6. Taking the wild-type (WD) modelled structure as a template, mutated protein structure was built and visualized using CHIMERA. The mutated protein structures for identified substitution mutations were compared with WD for the number of hydrogen bond interactions around the 5Å region of the mutated residue in CHIMERA (Fig.4). Impact on protein stability was predicted using DUET <http://marid.bioc.cam.ac.uk/sdm2/prediction> (DUET (unimelb.edu.au)), and protein conformation and flexibility was performed using DynaMut (<http://biosig.unimelb.edu.au/dynamut/prediction>, <http://biosig.unimelb.edu.au/dynamut/>). For intronic changes identified, the potential pathogenic effect for splice-site prediction was determined by varSEAK online tool <https://varseak.bio>.

Results:

Clinical and sequencing analysis.

CHED Familial case1– In this consanguineous family (denoted as F1), out of four siblings, three presented with a CHED clinical phenotype. All three affected siblings showed varying degrees of corneal clouding. As a part of current management for CD, all three cases underwent DSAEK surgery. The parents and unaffected children were found to be asymptomatic. Upon *SLC4A11* sequencing, a homozygous C to G DNA-nucleotide substitution was identified in all three affected cases at cDNA 1514 position of *SLC4A11*, leading to change of codon TCG to TGG (c.1514TCG>TGG), resulting in a change of amino acid serine to tryptophan at amino acid 489th

position (p.Ser489Trp). Parental analysis found both the parents as heterozygous for this mutation showing their carrier status **Fig.2(I)**. The change was absent in the fourth unaffected child (U1), and 80 healthy controls analysed.

CHED Familial case2– In this non-consanguineous family (denoted as F2) two siblings were affected. The younger girl presented with significant corneal clouding, while the older boy with a milder phenotype. Both parents had asymptomatic FECD phenotypes. Upon genetic analysis, both siblings were identified with compound heterozygous changes comprising substitution of A>C at cDNA 529 position and insertion of T at cDNA 2653 position **Fig.2(II)**. The former is a synonymous change without changing amino acid (p.Arg529Arg) while later creates a frameshift at Valine 805th position and generating a premature stop codon at 877th position, 15 amino acids before natural termination codon. Both the changes were absent in 80 healthy controls analyzed.

CHED Non-familial cases – Five cases (N1 to N5) with no familial history of diseases and single affected proband were sequenced to identify *SLC4A11* variations. Case-N1 presented with a bilateral decreased vision since birth and was identified with c.1487 G>T mutation, which was not reported and absent in 80 controls analyzed **Fig.2(iii)**. Case-N2 presented with a progressive decrease in vision with glaucoma. Case-N2 was identified with a homozygous substitution of A to G, two bases upstream of cDNA 620 position in the flanking intronic region at the beginning of exon 5 **Fig.2(iv)**. This change was unreported and excluded in 80 controls analyzed. Case N3 showed congenital white opacity along with glaucoma. Case-N3 was identified with a substitution mutation c.2653 C>T (p.Arg869Cys) previously reported in Indian CHED patients in two studies [3, 14] **Fig.2 (V)**. CHED cases N4, N5 did not show the presence of any pathogenic changes.

Mutational characterization - in silico analysis

c.1514TCG>TGG (p.Ser489Trp)

This novel mutation found in family-F1 had high penetrance and persistence of occurrence as it affected three kids in successive birth. The Ser489 position was highly conserved across 147 species. SIFT, PolyPhen composite score derived from Predicts SNP showed the mutation having deleterious effects. The homology-based Ser489Trp mutated *SLC4A11* protein structure was built, taking modeled *SLC4A11* WD as a template **Fig.3B**. The DUET protein stability score of the mutated protein showed a destabilizing effect, and the DynaMut score indicated restricted local flexibility as well. The number of hydrogen bond interactions around the 5Å region of the mutated residue was found to be decreased dramatically from 136 to 116 **Fig.4 (A1-A2)**.

c.1487G>T (p.Ser480Ile)

This novel mutation was found in case-N1 in a well-conserved region across 132 species. The Predict SNP score were deleterious. The mutated protein built showed decreased protein stability and local flexibility caused due to this mutation **Fig.3C**. The number of hydrogen bond interactions around the 5Å region of the mutated residue was found to be decreased from 15 to 13 **Fig.4 (B1-B2)**.

c.2653C>T (p.Arg869Cys)

This mutation was identified in sporadic case N3 and was previously reported to have an effect on the interaction of transmembrane helix with the cytoplasmic domain of the protein.[14]. The region is very highly conserved across 150 species. The SIFT, PolyPhen scores showed deleterious effects. The homology-based Arg489Cys mutated *SLC4A11* protein structure was built **Fig.3D**. The DUET protein stability score showed a destabilizing effect of the mutation, while DynaMut

score indicated increased local flexibility. The number of hydrogen bond interactions around the 5Å region of the mutated residue was found to be decreased from 15 to 13 **Fig.4 (C1-C2)**.

c.529A>C + c.2461insT (p.Arg161Arg + p.Val805fs)

This compound heterozygous change was shared between two siblings' familial case F2. Since the first component of mutation is a synonymous change, it is predicted that the combined effect of both mutations leads to an adverse event in protein structure.

c.620-2A>G

It was identified as a novel splice site variant, 2 bases upstream of exon 5 in sporadic CHED case N2. The varSEAK online tool predicted loss of function for authentic splice site at this position.

Fig.1

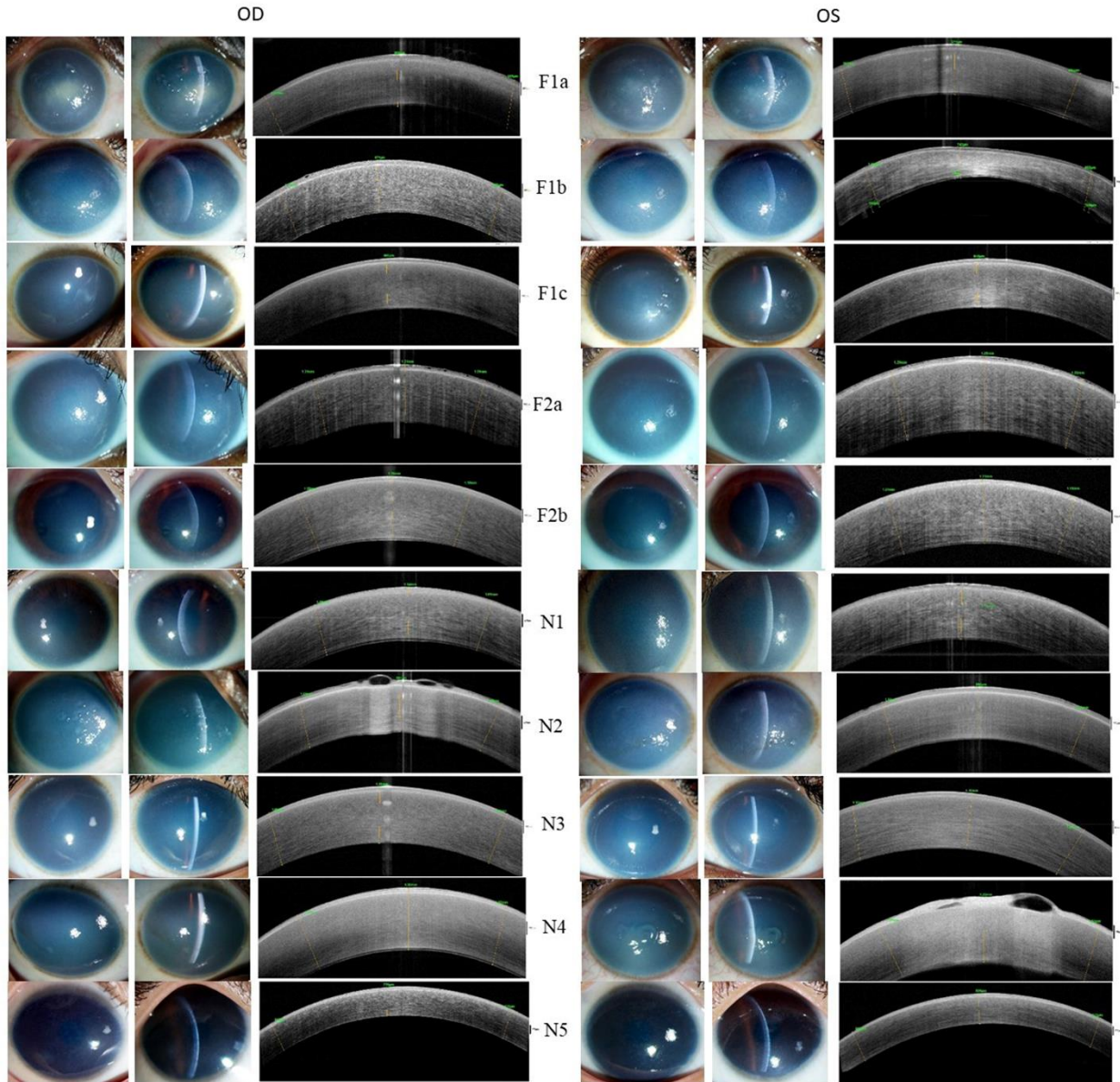


Fig. 1: Clinical slit lamp and Anterior Segment-Optical Coherence Tomography (AS-OCT) images of recruited cases

Left to right- Slit lamp images and AS-OCT images of the familial (F1,F2) and non-familial (N1-N5) CHED cases. Cloudy and hazy cornea is observed by slit lamp, OCT images indicated edematous haze in the individuals; OD- Right eye, OS- Left Eye.

Fig.2

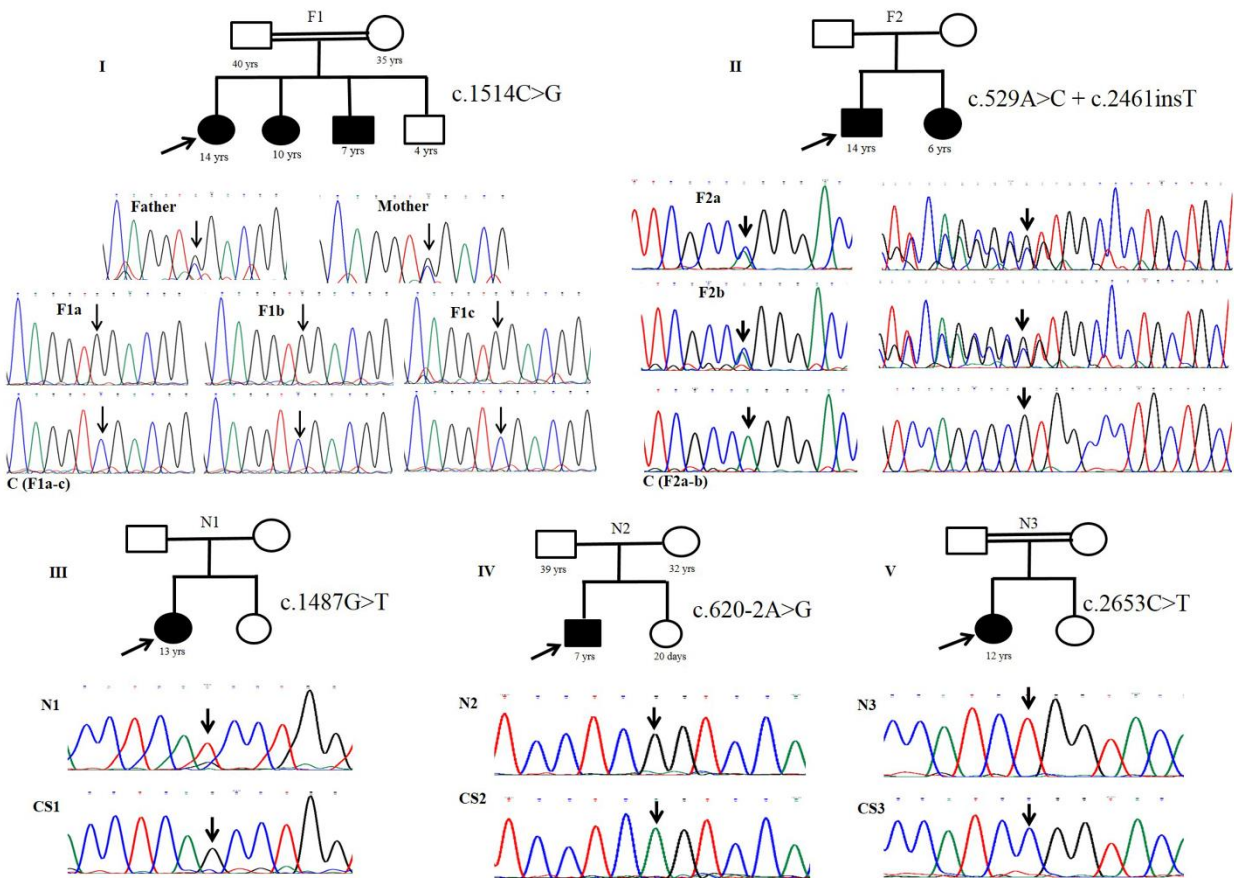


Fig. 2: Pedigree and Chromatogram of familial and non-familial CHED cases, identified with *SLC4A11* mutations.

(I-V) representative pedigree and their sequenced chromatogram for all subjects compared with wild type control chromatogram. I and II represent familial (F1,F2) case identified with hom. c.1514C>G (p.Ser489Trp) and com.het c.529A>C (p.Arg161Arg) + c.2461insT (p.Val805fs) mutations respectively. II, III, and IV represent non-familial (N1,N2,N3) identified with hom. c.1487G>T (p.Ser480Ile), hom. c.620-2A>G and hom. c.2653C>T (p.Arg869Cys) mutation respectively.

Fig.3

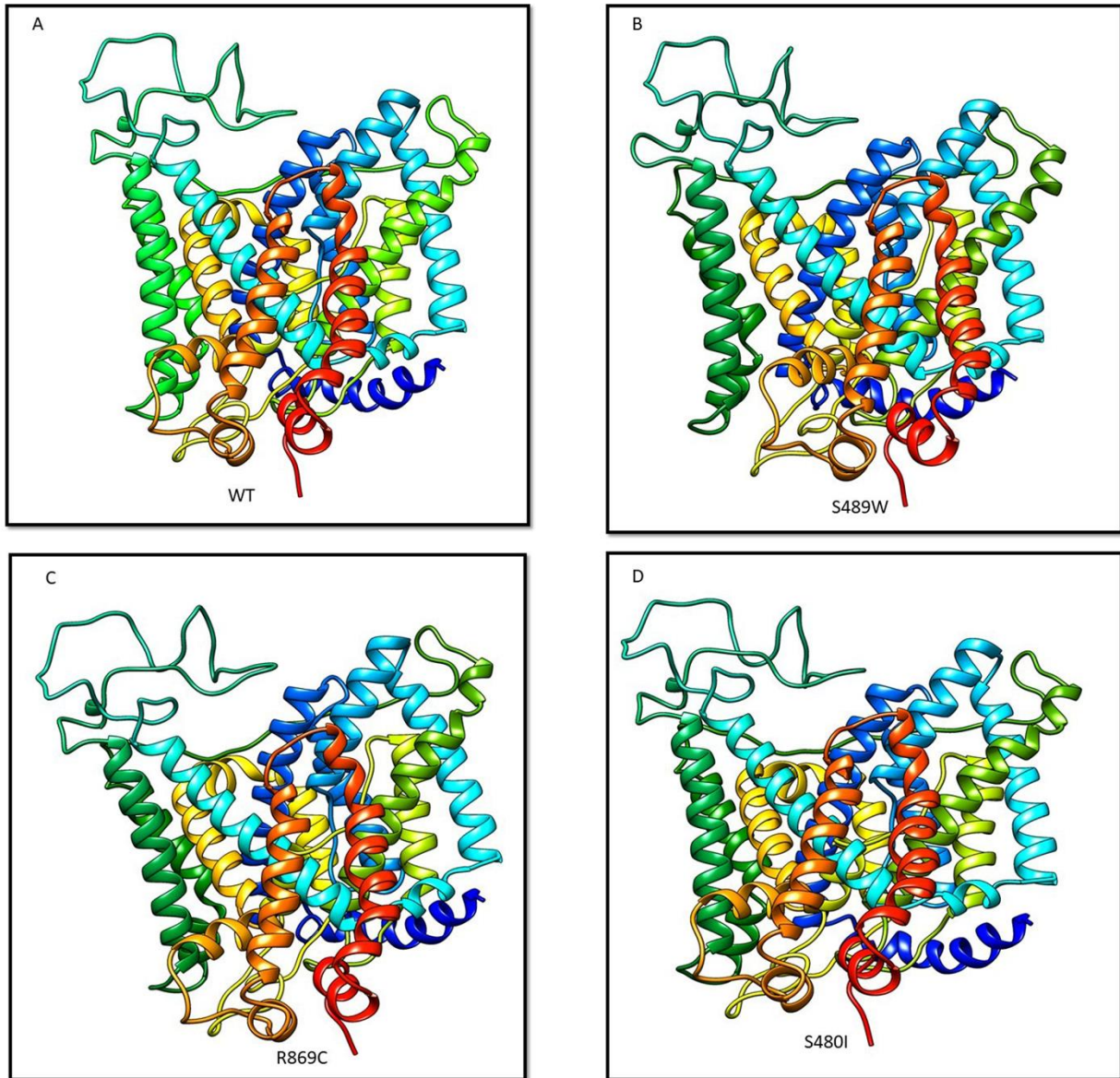


Fig. 3: Homology based protein modeling of WD and mutated SLC4A11 protein.

A – Wild type *SLC4A11* structure based on homology of structure of 4YZF PDB structure. Fig. B, C and D represent the mutated protein structure of S489W, R869C and S480I mutations respectively modelled taking WD as reference.

Fig.4

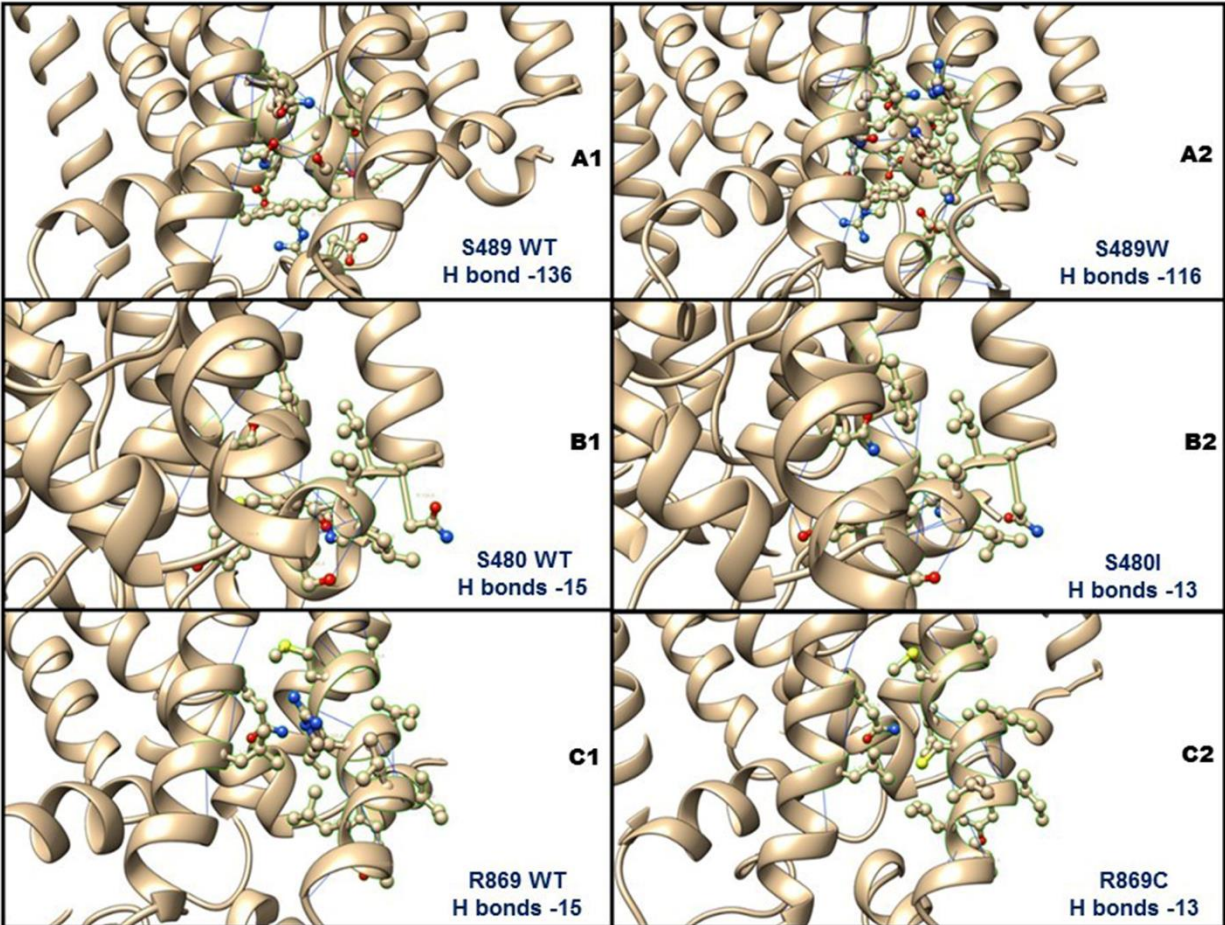


Fig.4: Mutational effect in hydrogen bond interactions around 5Å region of the mutation.

A1, **B1** and **C1** shows no. of H bonds of WT *SLC4A11* at S489, S480 and R869 position respectively, while **A2**, **B2** and **C2** shows corresponding no. of H bonds after it mutates to W489, I480 and C869 respectively.

Table 1: Details of recruited CHED cases in this study

CHED Case ID familial (F) and Non-familial (N)	Age group	Sex	Visual acuity		Corneal thickness (μm) OD/OS	Corneal opacity	Surgical interventions
			OD	OS			
F1a	Early adolescence	Female	CF 1m	CF CF	989/974	Severe	DSAEK+MMC
F1b	Middle childhood	Female	20/400	20/600	961	Moderate	DSAEK
F1c	Middle childhood	Male	20/600	20/600	986/940	Severe	DSAEK
F2a	Middle childhood	Female	20/800	20/800	1310/1280	Severe	DSAEK+MMC
F2b	Early adolescence	Male	20/160	20/200	1200/1210	Mild	DSAEK
N1	Early adolescence	Female	20/160	CF CF	1040/1110	Moderate/Severe	DSAEK
N2	Early adolescence	Female	20/800	20/800	967/995	Severe	DSAEK

N3	Middle childhood	Male	20/160	20/160	1080/1100	Moderate	DSAEK
N4	Early adolescence	Female	CF CF	CF CF	1200/1220	Severe	DSAEK
N5	Middle childhood	Male	20/400	20/500	781/776	Moderate	DSAEK

Table2: List of identified mutations in familial and non-familial CHED cases.

CHED Case familial (F) and Non-familial (N)	Case ID	Mutation identified (cDNA position)	Mutation identified (Protein position)	Exon /intro n locati on	Zygos ity	Parental /sibling status	Consang uinity	Literatur e Status
Family-1 (F1) (No. of affected =3)	F1a	c.1514C>G	p.Ser489Trp	Ex.12	Hom.	Carrier	Yes	Not Reported
	F1b	c.1514C>G	p.Ser489Trp	Ex.12	Hom.			
	F1c	c.1514C>G	p.Ser489Trp	Ex.12	Hom.			
Family-2 (F2) (No. of affected =2)	F2a	c.529A>C + c.2461insT	p.Arg161Arg + p.Val805fs	Ex.4 + Ex.17	Com. Het.	NA	No	Not Reported
	F2b	c.529A>C + c.2461insT	p.Arg161Arg + p.Val805fs	Ex.4 + Ex.17	Com. Het.			
Non-familial cases (N1-N5)	N1	c.1487G>T	p.Ser480Ile	Ex.11	Hom.			
	N2	c.620-2A>G	Splice variant	Int.4	Hom.	No	Not Reported	
	N3	c.2653C>T	p.Arg869Cys	Ex.18	Hom.	Yes	Reported	

	N4	-Ve	-Ve	--	--		No	--
	N5	-Ve	-Ve	--	--		No	--

Table 3: in silico analysis of the identified SLC4A11 mutations

Sr. No.	Mutation Identified	Residue Conserveness score (ConSurf)	Pathogenicity Score (Predict SNP pathogenicity %) [SIFT PolyPhen2 score]					Homology modelling based analysis			
			Predict SNP	Ph. D SNP	Poly Phen 2	SIFT	SNA P	H-bond interactions (5A region around the mutation site)	Protein Stability (DUE T)	Protein local flexibility (DynaMut)	
1	c.1514C>G (p.Ser489Trp)	Highly conserved across 147 species SCORE=9	72%	82%	81% [1]	53% [0.00 2]	81%	Decreased from 136 to 116	$\Delta\Delta G$: : -0.516 kcal/mol ol (Destabilizin g)	$\Delta\Delta S_{vib}$ EN CoM: - 1.717 kcal.mol ⁻¹ .K ⁻¹ (Decrease of molecule flexibility)	
2	c.1487G>T (p.Ser480Ile)	Highly conserved	87%	88%	81% [1]	79%	81%	Decreased from 15 to 13	$\Delta\Delta G$: -0.17 (Destabilizin g)	$\Delta\Delta S_{vib}$ EN CoM: - 0.557	

		across 132 species				[0.003]			bilizin g)	kcal.mol ⁻¹ .K ⁻¹ (Decrease of molecule flexibility)
3	c.2653C>T (p.Arg869Cys)	Highly conserved across 150 species SCORE=8	87%	82%	81% [1]	79% [0]	85%	Decreased from 15 to 13	$\Delta\Delta G$ -1.012 kcal/mol (Destabilization)	$\Delta\Delta S_{vib}$ EN CoM: 0.188 kcal.mol ⁻¹ .K ⁻¹ (Increase of molecule flexibility)
4	c.620-2A>G	--	--	--	--	--	--	--	--	--
5	c.529A>C (p.Arg161Arg) + c.2461insT (p.Val805fs)	--	--	--	--	--	--	--	--	--

SIFT score – 0-0.05 deleterious; 0.05-1 tolerated

PolyPhen2 score- 0-0.05-benign, 0.15-0.85 possibly damaging, 0.85-1- damaging

Discussions

Ever since the *SLC4A11* gene was established as a causative gene for CHED-related phenotype, many pathogenic changes have been identified for its cause. Most of these variations are single base substitutions in coding regions. Changes like compound heterozygous or intronic changes are identified when a large set of cases are analysed. In this study, we could identify a spectrum of changes in a small set of CHED cases, of which 80% were novel signifying a wide range of mutations could be involved in CHED pathogenesis. The novel mutation p.Ser489Trp identified in family 1 (F1) showed different grades of severity of the disease among three affected members despite having identical changes. This shows different expressivity of *SLC4A11* mutation in similar genetic backgrounds. In our study, family 2 (F2) carried a compound heterozygous change with a synonymous Arg to Arg change. How a synonymous change with a combination of non-synonymous change in the form of compound heterozygosity could lead to disease pathogenicity is a matter of further investigation. The compound heterozygous mutation had a severe effect on one sibling while a mild impact on the other, thus again showing different expressivity. The carrier parents in F2 showed marginal FECD phenotype. This finding aligns with our previous publication where carrier parents in autosomal recessive CHED families may reflect the FECD phenotype [15]. The homology-based protein modeling provides a better platform to analyze the physiochemical changes caused due to mutations at various levels of structural analysis. In the absence of known crystal structure of *SLC4A11*, it has been applied as an alternative to analyze mutational effects[16]. In silico analysis showed that identified novel p.Ser489Trp mutation significantly decreased H-bond interactions around the mutational coordinate. Such changes in H bonds may considerably impact the 3D confirmation of protein. The other identified substitution mutations had a marginal decrease in H bond interactions. During structural analysis, the impact of mutations

was also reflected in protein flexibility and stability, which were compromised. The identified mutations in our study, positioned at conserved regions and had deleterious effects. In our study, two cases were negative for *SLC4A11* mutations. Few previous studies had similar consequences in their studies. Study done by Hemadevi B et al, 9 out of 20 families of Indian origin did not show mutations in coding regions as well as in the promoter region of the *SLC4A11* gene [17]. All nine members of a large multi consanguineous marriage CHED family from Saudi showed the presence of p.Thr271Met mutation except an affected twin family, which did not show the presence of a pathogenic mutation. [18]. In another study, nine out of 25 CHED families from north India were characterized with *SLC4A11* mutations, while the remaining 11 families were found negative for the presence of *SLC4A11* mutations [19]. These studies, including ours, emphasize the involvement of other genes or genetic mechanisms in CHED pathogenesis. In a recent study, exome sequencing for a single patient not detected with *SLC4A11* mutation, a mutation in *MPDZ* was identified as a possible causative gene [20]. However, such evidences are limited and needs further studies for proper conclusions. The absence of *SLC4A11* mutations in such studies could also be due to lack of accurate differential diagnosis. In addition, more studies are needed to establish a candidate genes or genetic mechanisms in CHED not carrying *SLC4A11* mutations.

Conclusions: Overall, our study contributed to CHED mutational spectrum adding four novel mutations and confirming a previously reported mutation in two familial cases and three non-familial cases. Our analysis also emphasizes the involvement of other genes or genetic mechanisms or clinical diagnosis for *SLC4A11* negative CHED cases. These finding may help in future planning in gene editing correction for reverting these mutation for the better management in CHED cases.

List of abbreviations: CHED, SLC4A11, FECD, PPCD, PPMD, CDPD, ASOCT, IC3D, HS, NSAID, CRISPR, BPA,

Declarations:

Ethics approval and consent to participate: The study was approved by the "Institutional Review committee for protection of research risk to humans, Indian Statistical Institute, 2015". Written informed consent from all adult participants and legal guardians/parents for minors were obtained for the research study. and publications. Competing interests

Consent for publication. Consent for publications were included in consent form

Availability of data and materials: All patient data has been anonymized, and any further information may be obtained from corresponding author.

Competing interests: The authors declare that they have no competing interests

Funding: The authors wish to thank the Indian Council of Medical Research (ICMR) for fellowship [Ref. No. 3/1/3/JRF-2019/ HRD (LS)/25389] and Hyderabad Eye Research Foundation (HERF) for financial and infrastructure support.

Authors' contributions: Mohd Salman and Anshuman Verma contributed equally for design and implementation of study along with manuscript preparation. Sunita Chaurasia helped in patient recruitment and clinical analysis. Muralidhar Ramappa contributed patient clinical data analysis as well supervision of work and manuscript writing. Dr Vivek Singh helped in study design, coordination and supervision. Deeksha Prasad contributed in experiments and, Chitra Kannabiran contributed in genetic analysis and manuscript writing

Acknowledgements: We would also like to thank all our patients and control individuals who gave consent and participated in this study.

Authors' information (optional)

References:

1. Neelam S, Mehta JS, Vithana EN, Mootha VV. Genetics of Corneal Endothelial Dystrophies: An Asian Perspective. In *Advances in Vision Research, Volume I 2017* pp. 353-361. Springer, Tokyo.
2. Jeang LJ, Margo CE, Espana EMJEER. Diseases of the corneal endothelium. 2021;**205**:108495
3. Vithana EN, Morgan P, Sundaresan P, et al. Mutations in sodium-borate cotransporter SLC4A11 cause recessive congenital hereditary endothelial dystrophy CHED2. 2006;**387**:755-57
4. Han SB, Ang H-P, Poh R, et al. Mice with a targeted disruption of Slc4a11 model the progressive corneal changes of congenital hereditary endothelial dystrophy. 2013;**549**:6179-89
5. Seitz B, Lisch W, Weiss JJKMfA. The revised newest IC³D classification of corneal dystrophies. 2015;**2323**:283-94
6. Patel SP, Parker MDJBri. SLC4A11 and the pathophysiology of congenital hereditary endothelial dystrophy. 2015;**2015**
7. Desir J, Moya G, Reish O, et al. Borate transporter SLC4A11 mutations cause both Harboyan syndrome and non-syndromic corneal endothelial dystrophy. 2007;**445**:322-26
8. AlArrayedh H, Collum L, Murphy CCJBJoO. Outcomes of penetrating keratoplasty in congenital hereditary endothelial dystrophy. 2018;**1021**:19-25
9. Zahra A, Dong Q, Hall M, et al. Identification of Potential Bisphenol A BPA Exposure Biomarkers in Ovarian Cancer. 2021;**109**:1979

10. Alka K, Casey JRJIo, science v. Ophthalmic nonsteroidal anti-inflammatory drugs as a therapy for corneal dystrophies caused by SLC4A11 mutation. 2018;**59**10:4258-67
11. Shyam R, Ogando DG, Kim ET, Murugan S, Choi M, Bonanno JAJOS. Rescue of the Congenital Hereditary Endothelial Dystrophy Mouse Model by Adeno-Associated Virus–Mediated Slc4a11 Replacement. 2022;**21**:100084
12. Uehara H, Zhang X, Pereira F, et al. Start codon disruption with CRISPR/Cas9 prevents murine Fuchs’ endothelial corneal dystrophy. 2021;**10**:e55637
13. Lohia A, Sahel DK, Salman M, et al. Delivery Strategies for CRISPR/Cas Genome editing tool for Retinal Dystrophies: challenges and opportunities. Asian Journal of Pharmaceutical Sciences 2022
14. Jiao X, Sultana A, Garg P, et al. Autosomal recessive corneal endothelial dystrophy CHED2 is associated with mutations in SLC4A11. 2007;**44**1:64-68
15. Chaurasia S, Ramappa M, Annapurna M, Kannabiran CJC. Coexistence of congenital hereditary endothelial dystrophy and Fuchs endothelial corneal dystrophy associated with SLC4A11 mutations in affected families. 2020;**39**3:354-57
16. Zahra A, Hall M, Chatterjee J, Sisu C, Karteris EJJOMS. In Silico Study to Predict the Structural and Functional Consequences of SNPs on Biomarkers of Ovarian Cancer OC and BPA Exposure-Associated OC. 2022;**23**3:1725
17. Hemadevi B, Veitia RA, Srinivasan M, et al. Identification of mutations in the SLC4A11 gene in patients with recessive congenital hereditary endothelial dystrophy. 2008;**12**65:700-08
18. Shah SS, Al-Rajhi A, Brandt JD, et al. Mutation in the SLC4A11 gene associated with autosomal recessive congenital hereditary endothelial dystrophy in a large Saudi family. 2008;**29**1:41-45

19. Paliwal P, Sharma A, Tandon R, et al. Congenital hereditary endothelial dystrophy-mutation analysis of SLC4A11 and genotype-phenotype correlation in a North Indian patient cohort. 2010;**16**:2955

20. Moazzeni H, Javadi MA, Asgari D, et al. Observation of nine previously reported and 10 non-reported SLC4A11 mutations among 20 Iranian CHED probands and identification of an MPDZ mutation as possible cause of CHED and FECD in one family. 2020;**10411**:1621-28

Supplementary Table1: List of identified mutations reported in *SLC4A11* in CHED/FECD phenotype

Mutations	AA Change	Exons	Ethnic origin	Clinical Phenotype	Reference
c.2264G>A	p.R755Q	17	Myanmar	CHED2	Vithana, Morgan, et al. 2006
c.1466C>T	p.S489L	12	Pakistan		
c.1391G>A	p.G464D	11			
c.1813C>T	p.R605X	14	India		
c.353_356delAGAA	Framshift 11 residue stop	4			
c.2605C>T	p.R869C	18			
IVS15 -6-16 del ins ggccggccgg	Splice site acceptor inactivation	Intron 15			
g.2943delTTinsA	p.Arg82ArgfsX33	2			
g.3552G>A	p.Ala160Thr	4			
g.8118delCT	p.His568HisfsX177	13			

g.8298C>T	p.Arg605X	14			
g.8379G>T	p.Glu632X	14			
g.9044G>A	p.Arg755Gln	17			
Hom g.9191G>A	p.Arg804His	17			
Hom g.9200delTinsGG	p.Leu807Arg	17			
Hom g.9361C>T	p.Thr833Met	18			
Hom g.9469G>A	p.Arg869His	18			
Hom c.859_862delGAGainsC CT	Frameshift	8			Kumar, Bhattacharjee, et al. 2007
Hom c.2014_2016delTTC	In frame deletion	15			
CompHet c.743G>A +C.1033A>T	p.Ser232Asn p.Arg329X	+ 6 +7	Chinese- American		Aldave, Yellore, et al. 2007
c.473_480del GCTTCGCC	Frameshift	4	Gipsy Eastern Europe)		
c.1378_1381del TACGinsA)	p.Tyr460_Ala461 delinsThr	11	Dominica n Republic	Harboyan syndrome	Desir Julie et al. 2007
c.1463G>A	p.Arg488Lys	11	Morocco		
c.2233_2240dup TATGACAC) c.2528T>C)	p.Thr747ThrfsX6 + p.Leu843Pro	16	South American Indian		

c.2423_2454del32nt+ c.2528T>C	p.Leu808ArgfsX 110 + p.Leu843Pro	18	Netherlan ds				
c.637T>C + c.2566A>G	p.Ser213Pro+ p.Met856Val	5+18	Sephardi Jewish				
c.2470G>A	p.Val824Meth	18	India	Non- syndromic CHED			
c.427G>A	p.Glu143Lys	4					
c.1156T>C	p.Cys386Arg	9					
c.2263C>T	p.Arg755Trp	17					
c.720G>A	p.Trp240X	6					
c.2240+1G>A	Splice site	Intron 16	UK	CHED2	Ramprasad et al., 2007		
c.2398C>T + c.2437- 1G>A	p.Gln800X + Splice acceptor inactivation	Ex17 + Intron17					
Hom c.654-97)_C.778 -1488)del698bp	Frameshift	6	India				Hemadevi, Veitia et al. 2008
Hom c.2318C>T	p.P773L	17					
Hom c.473_480 delGCTTCGCCinsC	p.Arg158ProFSX3	4					
Hom c.2618T>C	p.L873P	19					
CompHet c.2318C>T + c.2506C>T	p.P773L+ p.Q836X	17 +18					

c.806C>T	p.A269V	7			
c.478G>A	p.A160T	4			
c.1156T>C	p.C386R	9			
c.374G>A	p.R125H	4			
c.2263C>T	p.R755W	17			
c.271C>T	p.Thr271Met	6	Saudi		Shah, Al-Rajhi, et al. 2008
c.2126G>A	p.Gly709Glu	16	Chinese	FECD	Vithana, Morgan, et al. 2008
c.2261C>T	p.Thr754Met	17			
c.99_100delTC	p.S33SfsX18	1			
c.1195G>A	p.Glu399Lys	9	India		
c.520delGCTTCGCC	p.Arg158fs	4	Saudi	CHED2	Aldahmesh, Khan, et al. 2009
c.1228G>C	p.Gly394Arg	9			
c.1253G>A	p. Gly418Asp	10			
c.1044+25 del19nt	Intronic mutation	7			
c.2236C>T	p.Arg757X	16			
c.2114+1G>A	Splice site	15			
c.2240+1G>A	Splice site termination	16 splice region)	India		Paliwal, Sharma, et al. 2010
c.2470G>A	p.Val824Met	18			
c.2518-2520delCTG	p.Leu480 del	18			
c.1156T>C	p.Cys286Arg	9			
c.2470G>A	p.Val824Meth	18			
c.501G>C	p.E167D	4		FECD	

c.845G>C	p.R282P	7	Northern Europe	CHED2	Riazuddin, Vithana et al. 2010
c.1577A>G	p.Y526C	13			
c.1723G>A	p.V575M	13			
c.1748G>A	p.G583D	13			
c.2224G>A	p.G742R	16			
c.2500G>A	p.G834S	18			
c.1831T>C	p.Cys611Arg	14	India	CHED2	Kodaganur, Kapoor, et al. 2013
c.1249 G>A	p.Gly417Arg	11			
c.2170 C>G	p.His724Asp	16			
c.785C>T	p.Thr262Ile	8			
c.1391G>A	p.G464D	11	Pakistan	CHED2	Siddiqui, Zenteno et al. 2014
c.397T>C	p.F133L	4	Mexican		
c.1158C>A	p.C386*	9	Korean	CHED2	Kim, Ko et al. 2015
c. 1156T>C +	p.Cys386Arg +	9 +	India		
c. 1244G>A	p.Ser415A	10			
c.150T>A	p.C50X	1	Iran	CHED2	Moazzeni, Javadi et al. 2019
c.586G>T	p.D196Y	4			
c.1217A>T	p.D406V	9			
c.1245delC	p.S415RfsX15	9			
c.1307C>T	p.A436V	10			
c.1537+1G>C	Splice site	12			
c.1606A>T	p.S536C	13			
c.2117T>A	p.I706N	16			
c.2328 delT	p.L776LfsX72	17			

c.2519T>C	p.L840P	18			
c.433G>A	p.Asp129Asn	4	India	CHED2	Chaurasia, Ramappa et al. 2020
c.9361C>T	p.Thr833Met	18			
c.9191G>A	p.Arg804His	17			
c.1249 G>A	p.Gly417Arg	11			
c.2470G>A	p.Val824Met	18			
c.1466C>T	p.Ser489Leu	12			
c.382C>T	p.Arg112X	4			
c.1813C>T	p.Arg605X	14			

Supplementary Table2: Primer list and PCR annealing temp. for each amplicon of *SLC4A11*

Amplicon No.	Exon	Primer Sequence		Annealing Temp (°C)	Amplicon size (bp)
Amplicon 1	Exon 1	FP	TGAGATTAAGGCTGGCTT CC	64	298
		R P	CTTTTGCCCGACAAGCTCT		
Amplicon 2	Exon 2-3	FP	CGAGAGTGGGACAGTCCA G	66	497
		R P	AGGGAAGCCATCACCTCA G		
Amplicon 3	Exon 4-5	FP	GGCCCGTGTGGTTCTGTC	66	494
		R P	ACAGGGGACATGGGACAC		
Amplicon 4	Exon 6	FP	CAAGGTTCGAGGGGGTTCT	66	351
		R P	GTTTCTGACACACCCACA GG		
Amplicon 5	Exon 7-8	FP	GGGAGAGCACCTTCACCT G	64	556
		R P	GGATGGGAGAGAGGGTTT GCT		

Amplicon 6	Exon 9-10	FP	ACTGATGGTACGTGGCCT CT	64	567
		R P	CGTCCATGCGTAGAAGGA GT		
Amplicon 7	Exon 11-12	FP	CATTGGTGATTCTGCTGAC C	66	696
		R P	ACTCAGCTTGAGCCAGTC CT		
Amplicon 8	Exon 13-14	FP	GAGCCCTTTCTCCCTGAGA T	64	623
		R P	GGTTGTAGCGGAACTTGC TC		
Amplicon 9	Exon 15	FP	GCCTTCTCCCTCATCAGCT C	66	399
		R P	GTAGGCAGTGCCCTTCAC C		
Amplicon 10	Exon 16	FP	AATGCACCGGAGAACAGG T	66	389
		R P	CCGCGAGTGTCACCTCTG		
Amplicon 11	Exon 17	FP	CGTGGACCCTGAGGAGTG	62	420
		R P	CCCTCCGGATGTAGTGTGT C		
Amplicon 12	Exon 18	FP	CTCGATGGCAACCAGCTC	66	452
		R P	CTAGGCAGGACCCCTCCT C		
Amplicon 13	Exon19	FP	GGTGTCCACTGCCTTCTCT C	64	341
		R P	AACGCTCTTGGCCTAAAG CT		